

From spectral fluctuations to acoustic response of a soft interface using the second law

Shamit Shrivastava¹, Robin O. Cleveland¹, Matthias F. Schneider²,

1. Institute for Biomedical Engineering, University of Oxford, Oxford OX3 7DQ, UK

2. Medizinische und Biologische Physik, Technische Universität Dortmund, Otto-Hahn Str. 4, 44227 Dortmund, Germany

Physical and/or chemical changes in biological interfaces can be quantified by corresponding changes in the thermodynamic state of the interface. Based on Einstein's approach to thermodynamics, we show that fluorescence spectra of a dye embedded in a lipid membrane is a function of the state of the interface. We derive the coupling between the energy fluctuations of a fluorophore and its environment allowing the thermodynamic susceptibility, in particular, the specific heat of the interface to be estimated from the spectra of the embedded fluorophore. The estimate of the thermodynamic susceptibility is shown to hold not only for quasi-static near-equilibrium measurements, but also for dynamic state changes in lipid vesicles induced by broadband pressure impulses of the order of 1MPa peak amplitude and 10 μ s pulse duration. These experiments also provide crucial insights into how dynamic state changes may affect biological function, for example, during an action potential or during therapeutic use of acoustic impulses in the form of ultrasound or shock waves.

Introduction

The solvation environment of proteins and enzymes play a critical role in their function [1–4]. Biological membranes integrate enzyme and proteins that perform synergistically and as such membrane-protein systems present a unique challenge in understanding how the state of the system might affect the function of embedded molecules. Microscopically, proteins function in a probabilistic manner and therefore in order to understand the relation between various environmental cues and protein activity, it is necessary to understand the coupled fluctuations during membrane-protein interaction [5,6]. Thus for example in order to determine pressure dependent channel currents, pressure fluctuations are important and not the mean pressure. The importance of the susceptibility (dielectric) of the hydration shell and its relation to fluctuations in protein dynamics has been previously highlighted by Fraunfelder [1,2] and Marcus [3,4]. However, by the extension of this logic to molecules that belong to a larger interface, such as a biological membrane, the fluctuations of a hydrated protein system can in turn be dominated by the fluctuations of the larger membrane interface, as the interface has its own entropy potential [7]. From a thermodynamic perspective, the macroscopic responses [8–10] as well as the microscopic fluctuations [11,12] of any observable of the interface have to conform to the entropy potential of the interface in order to satisfy the second law. Therefore, instead of constructing a membrane-protein system one interaction at a time, we ask the inverse. Can we *impose* the second law as a *principle* on to the molecules embedded in the system and make useful and general prediction about their equilibrium and dynamic behavior?

Fluorescent molecules known as “solvato-chromic” dyes such as Laurdan, Prodan and di-4-anepdhq [13–27] as well as “electro-chromic” (voltage sensitive) dyes such as di-8-anneps and RH421 [28], are known to have spectral properties that are sensitive to their dielectric environment. These dyes are designed to exhibit a high ground state and/or transition dipole moments compared to otherwise “non-sensitive” probes and as a result do significantly more work in a dielectric environment. This results in an environment sensitive shift in the absorption and emission spectrum of these dyes. In this study we employ Laurdan, which shows a red shift as the membrane becomes more hydrated and has been used extensively in membrane studies (Table 1). We show that such dyes can be used to determine how the local energy landscape, as inferred from their fluorescence spectrum, is affected by a macroscopic change in the thermodynamic state of

the membrane. The finding is shown to be consistent with experimental studies from the literature. Furthermore, the relation also allows direct estimation of local thermodynamic properties of the system from steady state fluorescence measurements. Although the relationship is derived for near equilibrium perturbations, we further show experimentally that it can be used under dynamic condition as well, by predicting spectral shift during acoustic impulses, assuming local equilibrium.

Entropy potential for a dye-membrane system

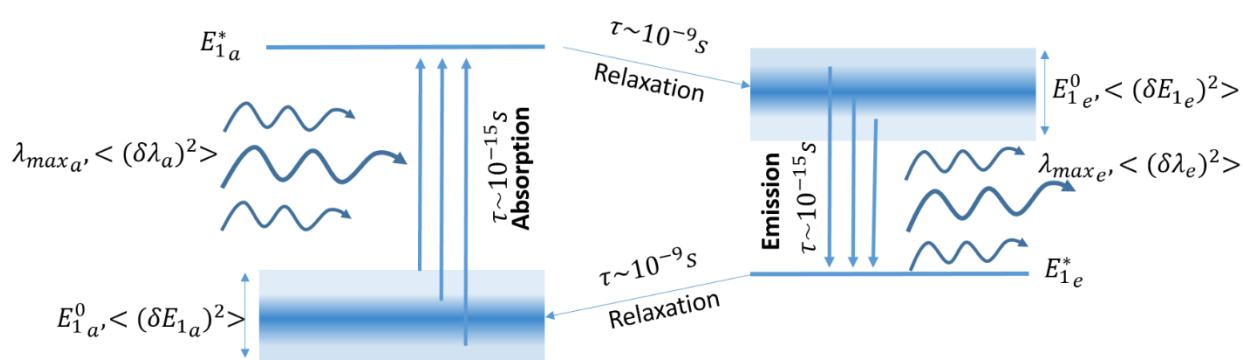


Figure 1 Approximate representation of fluorescence absorption and emission. *The schematic outlines how the variations in the photon wavelengths $\langle (\delta\lambda)^2 \rangle$ during absorption or emission process are related to the variations $\langle (\delta E_1)^2 \rangle$ in the ground state energy E_1^0 of the fluorophore. For absorption the ground state dipole of the fluorophore is in equilibrium with the environment, while for emission the ground state transition dipole is assumed to have reached an equilibrium with its solvation shell [14]. The excited states E_1^* immediately upon absorption or emission is assumed to be independent of solvent relaxation phenomenon (see text). The subscript ‘a’ and ‘e’ for absorption and emission respectively, have been dropped in main text for the sake of simplicity.*

The fluorescence phenomenon, even though represented by a single molecule in its local environment, is an ensemble property of the system. The energy of a photon that is absorbed or emitted represents the energy difference between the ground and excited states of the corresponding fluorophore that belongs to the ensemble. Hence the width of the spectrum of a fluorescence molecule depends strongly on the statistical distribution of states accessible to an ensemble during absorption or emission, which in turn should increase with an increase in conformational space (fig 1). When the dye belongs to a hydrated interface such as a lipid

membrane, this conformational space also includes various arrangements with lipid and water molecules that are allowed for the given macroscopic state of the entire system.

For a more fundamental description of the effects of thermodynamic perturbations, let E_1 be the internal energy of the dye (subsystem 1) which is in equilibrium with the interface and let E_2 be the energy of the rest of the interface (subsystem 2). The number of ways the total energy can be distributed in these two compartments is a function of the entropy of the entire system, given that the two systems interact and the individual probabilities are not independent, i.e. ($W(E_1, E_2) \neq W(E_1) \cdot W(E_2)$) [29]. Taking a heuristic point of view and noting that an interface has its own specific heat and entropy decoupled from the bulk [7], the entropy of the interfacial system is defined as $S(E_1, E_2)$ [30] which gives the probability distribution function as;

$$dW = K \cdot e^{S(E_1, E_2)} dE_1 dE_2 \quad (1)$$

where K is a constant. Realizing that the most probable energy state E_1^0 of the dye lies at the maximum of entropy potential, the Taylor expansion of the entropy up to second term near (E_1^0, E_2^0) can be written as;

$$S(E_1, E_2)_{E_1^0, E_2^0} = \frac{\partial S}{\partial E_1} \delta E_1 + \frac{\partial S}{\partial E_2} \delta E_2 + \frac{1}{2} \frac{\partial^2 S}{\partial E_1^2} (\delta E_1)^2 + \frac{1}{2} \frac{\partial^2 S}{\partial E_2^2} (\delta E_2)^2 + \frac{\partial^2 S}{\partial E_1 \partial E_2} \delta E_1 \delta E_2 \quad (2)$$

The derivatives are taken at $E_1 = E_1^0$ and $E_2 = E_2^0$. As there is an entropy maximum at (E_1^0, E_2^0) , we have $\frac{\partial S}{\partial E_1} = \frac{\partial S}{\partial E_2} = 0$ and using the definition of temperature $\frac{\partial S}{\partial E} = \frac{1}{T}$ and heat capacity $C = \frac{\partial E}{\partial T}$, where $\delta E_1 = E_1 - E_1^0$ and so on, eq.(2) can be reduced to [31];

$$S(E_1, E_2)_{E_1^0, E_2^0} = -\frac{1}{2} \left\{ \frac{(\delta E_1)^2}{C_1 T_1^2} + \frac{(\delta E_2)^2}{C_2 T_2^2} + \frac{\delta E_1 \delta E_2}{T_2^2} \frac{\partial T_2}{\partial E_1} \right\} \quad (3)$$

Where T has the units of energy. T_1 and T_2 represent the microscopic temperatures of the dye subsystem and environment, respectively. Note that, T_1 and T_2 acquire physical significance from the macroscopic measurements of temperature T only when the system is assumed to be in local equilibrium and hence $T_1 = T_2 = T$. Substituting eq.(3) into eq. (1) and comparing the coefficients with a Gaussian distribution, the energy fluctuations in the two systems do not only depend on the heat capacities of the respective systems

$$\langle (\delta E_i)^2 \rangle \sim C_i T_i^2 \quad (i = 1 \text{ or } 2), \quad (4a)$$

but are also coupled

$$\langle \delta E_1 \delta E_2 \rangle \sim T_2^2 \left(\frac{\partial T_2}{\partial E_1} \right)^{-1} \quad (4b)$$

Going back to the fluorophore membrane system, if E_1 is the (internal) energy of the dye (subsystem 1), it is directly related to the mean radiation energy E_r absorbed or emitted by the fluorophore as per the first law;

$$|E_1^* - E_1| = E_r(\lambda) \quad (5)$$

Here E_1^* is the energy of the electronic state immediately upon absorption or emission which is essentially instantaneous ($\sim 10^{-15}$ sec) [32] and can be assumed to be independent of any rearrangement in hydration shell ($\sim 10^{-9}$ sec) [14,33] where λ is the wavelength of radiation. Therefore any variation in $E_r(\lambda)$ due to rearrangement of the hydration shell can be attributed mainly to variations in E_1 , i.e. only the relaxed state energy distribution of the dye molecules¹. From Maxwell theory, the spectrum ρ_λ (radiation density) and the corresponding mean radiation energy absorbed or emitted $E_r(\lambda)$ are related as [34]

$$E_r(\lambda) = \frac{L^3 \lambda^2}{8\pi c^2} \rho_\lambda \quad (6)$$

For the emission process, if λ_{max} is the observable that determines the state phenomenologically based on Einstein's description of the entropy potential, then differentiating eq. 6 and substituting in eq. 5, also using $\left(\frac{d\rho_\lambda}{d\lambda} \right)_{\lambda_{max}} = 0$ and for a normalized distribution ($\rho_{\lambda_{max}} = 1$), we have $\delta E_1 \sim \delta E_r \sim \lambda_{max} (\delta \lambda_{max})$. Now either by propagating the error in $E_r(\lambda)$ to λ , or by redefining the

¹ Since we are interested in fluctuations in E_1 , E_1^* is assumed constant for the simplicity of analytical results. In general an increase in the distribution of the radiation would result from addition of the increase in distributions of both the ground and the excited states of the dye molecules $\delta E_1^{*2} + \delta E_1^2 = \delta E_r^2$, (properly $S(E_1, E_1^*, E_2)$ written for steady state) as a result of change in the state of the hydration layer. Thus an increase in distribution of radiation still reports an increase in fluctuations of the hydration layer and the assumption regarding E_1^* , although justified by the timescales, is not necessary.

entropy potential phenomenologically as $S(\lambda_{max}, E_2)$ (Kaufmann, 1989) and using eq.(4), (5), (6) following relation can be derived after dropping the constants

$$\langle \delta\lambda_{max}\delta E_2 \rangle \sim T^2 \left(\frac{\partial T_2}{\partial \lambda_{max}} \right)^{-1} \quad (7)$$

Here $\delta\lambda_{max}$ is the fluctuation or perturbation in the wavelength of radiation absorbed or emitted by the ensemble of dye molecules (subsystem 1), which is coupled to the fluctuations or perturbation δE_2 of the membrane (for instance due to a pressure impulse) via the state dependent coupling parameter $\left(\frac{\partial T}{\partial \lambda_{max}} \right)^{-1}$ which is experimentally accessible (λ_{max} corresponds to peak of the entropy potential obtained quasi-statically and hence $T_1 = T_2 = T$) and is essentially the change in mean or peak absorption or emission wavelength.

The term is plotted as function of temperature in fig. 2 for DPPC MLVs and shows strong correlation with the specific heat C [35] allowing us to write

$$\left(\frac{\partial T}{\partial \lambda} \right)^{-1} \sim C \quad (8a)$$

$$\Delta\lambda_{max} \sim \Delta E_2 \quad (8b)$$

Thus the λ_{max} is directly correlated to the energy of the surrounding membrane and the strength of coupling is determined phenomenologically by the constants of proportionality in eq.(8). While correlation is certainly valid near the transition region, its general validity has been discussed previously in detail by others for fluctuation correlations in lipid systems [36–38]. Using eq (7) and (8) one can write;

$$C(T) = \varepsilon \Delta\Gamma/T \quad (9)$$

Where $\Delta\Gamma = \sqrt{\Gamma^2 - \Gamma_0^2}$ can be substituted by the experimentally observed *excess* FWHM from spectrums of Laurdan, plotted for DPPC in Fig.2 as reported by others [39], and ε is a phenomenological constant of proportionality and Γ_0 is the spectral width of the dye in vacuum due to its intrinsic specific heat. Then C_{local} as obtained from Laurdan spectrum is plotted in the inset (fig. 2) using $\varepsilon = 10 \text{ kJ} \cdot \text{mol}^{-1} \text{ nm}^{-1}$ and $\Gamma_0 \approx 50 \text{ nm}$ approximated as FWHM of Laurdan in n-hexane [40]. The obtained C_{local} predicts the macroscopic excess C_p accurately [11,37] when

the state changes from gel to the transition region, however it doesn't decrease as sharply as macroscopically measured C_p when moving to fluid state. There are only a few studies on accurate single phase specific heat measurements of lipids but the estimated specific heat profile is remarkably similar to quantum statistical C_p calculated previously [41] based on a hindered harmonic potential and might provide further insights into the observed microscopic nature of specific heat in lipid environment. For example, the effects of increased hydration on the energy distribution of embedded molecules due to formation of hydrogen bonds [42]. Note that strong coupling between the embedded molecule and the membrane has a significant impact not only on the embedded molecule but also on the membrane, which can alter the properties of the environment locally as well as globally [43].

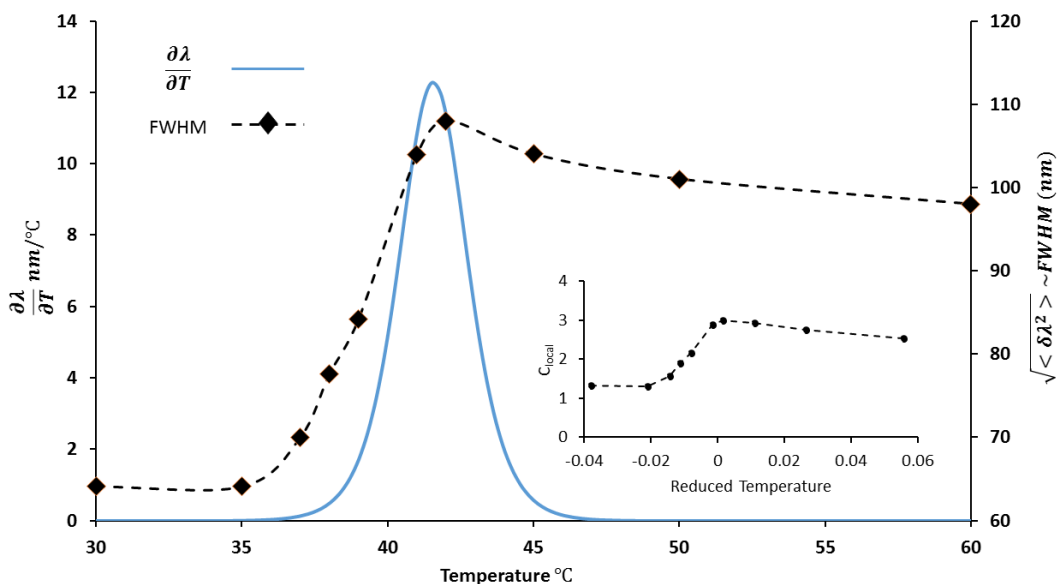


Figure 2 Estimating specific heat from observed emission spectrum of Laurdan *The rate of change of peak emission wavelength with respect to temperature $\frac{\partial \lambda}{\partial T}$ as obtained from reported emission spectrums in [39] is plotted as a function of temperature. From the same emission spectrum, FWHM was obtained and has been plotted on secondary axis. The inset shows the specific heat calculated purely from these optical measurements and using a constant fit parameter of proportionality.*

Given that solvent relaxation times are of the order of $\sim 10^{-9}$ s, eq. (7) and (8) can also be applied to a variety of dynamic processes at biologically relevant timescales, as the dye can be assumed in

local equilibrium. Hence for a dynamic perturbation, for example due to an acoustic impulse, the linear response of the system in terms of dynamic spectral shift in the emission should have the same relation to the specific heat (thermodynamic susceptibility in general) as the width of the spectrum. Next section shows this is indeed the case.

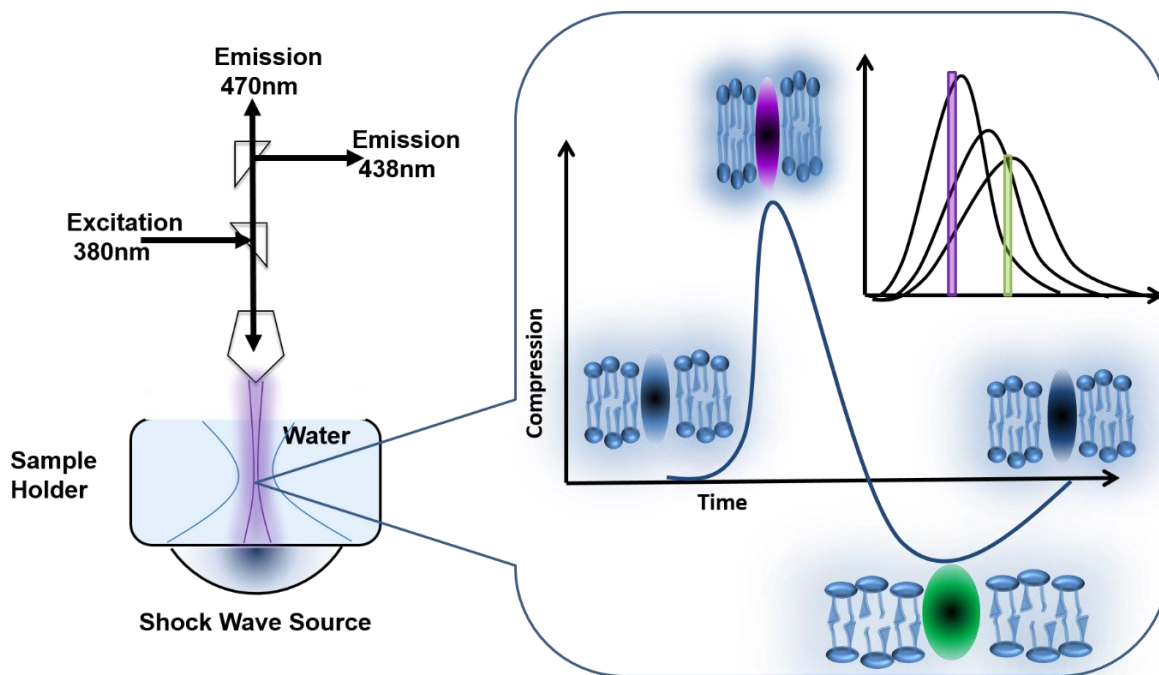


Figure 3 Experimental Setup A shock wave source coupled to a water tank provides the pressure impulse at its focus which coincides with the focus of the optical setup. The temperature controlled water tank has multilamellar lipid vesicles (MLVs), embedded with the dye Laurdan, present everywhere. As the pressure impulse interacts with the lipid vesicles, the emission spectrum shifts in opposite directions based on the state of the interface, as indicated in the schematic on the right. The shift is quantified ratiometrically by the two photomultiplier tubes recording simultaneously at two different wavelengths (438 and 470nm).

Materials and Methods

Materials:

The lipids 1,2-dioleoyl-sn-glycero-3-phosphocholine (DOPC 850375), 1,2-dimyristoyl-sn-glycero-3-phosphocholine (DMPC 850345), 1,2-dipalmitoyl-sn-glycero-3-phosphocholine

(DPPC 850355) were purchased as a 25 mg/mL solution in chloroform from Avanti Polar Lipids, Inc., Alabaster, AL, USA. Laurdan was purchased from Life technologies, USA. Unless otherwise stated, all other chemicals were purchased from Sigma Aldrich.

Preparation of multilamellar vesicles (MLVs):

100 μ l of the lipids (DOPC, DMPC or DPPC) (25mg/ml), from the chloroform stock without any further purification, were dried in a 10 ml glass vial overnight in a vacuum desiccator. The dried film was rehydrate in 5 ml MilliQ ultrapure water and heated for 30 mins on a hot plate at 50°C with the cap tightly sealed. The film was then vortexed at 2000 rpm for 30 seconds and the processes repeated once more to get the MLVs suspension. 1 μ l of a 50mg/ml solution of Laurdan in DMSO (dimethyl sulfoxide) was added to 5ml of MLV suspension, which was then mixed with 500ml of additional MilliQ water in the temperature regulated tank.

Optical and pressure measurements and data analysis:

A custom optical setup was built for dynamic fluorescence intensity measurements at two wavelengths (fig. 3). A high power light emitting diode (Thorlabs, M385LP1) was used as the excitation source with a central wavelength of 385nm followed by a bandpass filter (390 \pm 20nm). A dichoric mirror (414 nm) then separated the excited and emitted light, with the reflected light focused at the back focal plane of an objective (LWD M PLAN FL 20X Olympus) with a working distance of 13mm. The emitted fluorescence was split by another dichoric at 452 nm collected by two Hamamatsu photomultiplier tube (H10493-003) across two bandpass filters at 438 (\pm 12nm) and 470 nm (\pm 11nm). LED was triggered 5 ms before every acoustic impulse for a duration 10 ms.

A piezoelectric focused shockwave source (Swiss Piezoclast) was used to generate the acoustic impulse. The pressure waveform at the focus was measured using a needle hydrophone from Muller Instruments with a sensitivity of 12.5mV/bar (bandwidth 0.3 – 11 MHz \pm 3.0 dB). Shocks were fired at 3Hz repetition rate. Data was acquired using NI PCI 5122 dual channel simultaneous 100Ms/s digitizer for 500 μ s of which 50 μ s preceded the trigger and was analyzed using NI Labview.

Each waveform was averaged and sampled down to 5MHz. The first 10us were averaged to obtain I_0 for each channel. The overall waveform from each channel was normalized with respect to the corresponding base values to obtain relative intensity changes ($\frac{\Delta I}{I_0} = \frac{I}{I_0} - 1$). The relative change in ratiometric parameter ($\Delta RP/RP$) were obtained from the individual intensity changes, as in

$$\Delta RP/RP = \left(\frac{\Delta I}{I_0}\right)_{438nm} - \left(\frac{\Delta I}{I_0}\right)_{470nm}, \quad (10)$$

where $RP = I_{438nm}/I_{470nm}$. This minimizes extraneous signals, such as concentration inhomogeneities, background fluorescence and purely mechanical undulations in the field of view (motion of any surfaces in the experimental setup) that are otherwise inconsequential for the state of the lipid interface [44].

Spectral shifts during dynamic state changes

The pressure waveform to which the MLV suspension was subjected to is shown in figure 4a. The initial thermodynamic state of different MLV suspensions was quantified by the corresponding RP value (Fig 4b). DPPC with the main fluid-gel phase transition temperature as $T_{pt} = 41^\circ C$ [39] is in the most ordered state (RP=1.3) at $20^\circ C$ among the samples being tested. This can also be seen from the reduced temperature defined as $T^* = \frac{T-T_{pt}}{T_{pt}} = -0.067$, here temperatures are on an absolute scale. Similarly DMPC [45] with $T_{pt} = 23.4^\circ C$ set at $10^\circ C$, $23^\circ C$ and $37^\circ C$ represent successively more disordered states. DOPC with $T_{pt} = -20^\circ C$ [46] represents the most disordered at $20^\circ C$, with minimum RP among all the samples. As shown in figure 4b, reduced temperature allows us to represent different lipid formulations on the same temperature axis which shows direct correlation with the observed RP, underlining the significance of RP as an order parameter for the main gel-fluid transition in lipid systems. Indeed, given that significant temperature gradient were present in the water tank, the mean RP value is the reliable parameter here to define the mean state [38].

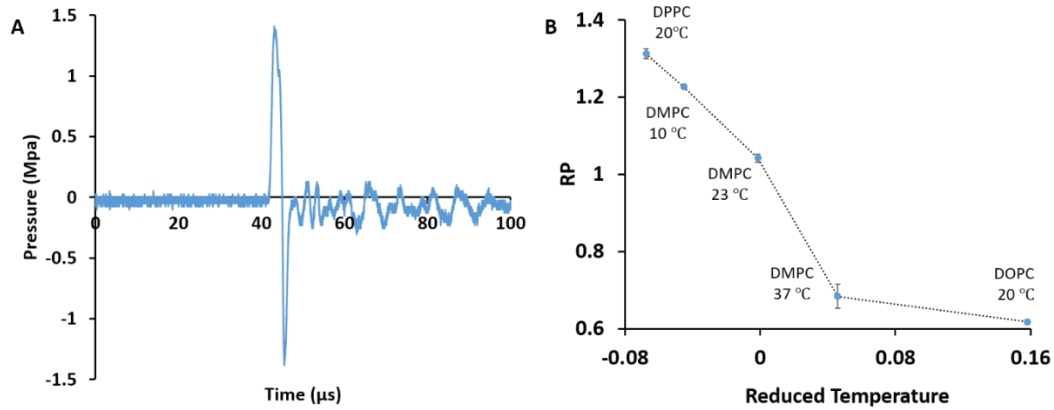


Figure 4 Applied pressure impulse and initial conditions (A) The waveform for the pressure impulse measured at the (peak pressures $\pm 1.30\text{Mpa}$). (B) The mean or equilibrium RP value calculated from Laurdan emission in different MLV formulations, plotted as a function of the respective reduced temperatures.

The response $\Delta RP / RP$, when these samples were subjected to pressure impulse (peak pressure $\pm 1.30\text{Mpa}$) is plotted as a function of state by first changing the temperature (fig.5). The impulse is fired at $t = 0\mu\text{s}$ and can be seen to arrive around $t = 50\mu\text{s}$ whenever the signal is significant. Only a negative response is observed with the maximum response of $\Delta RP / RP \approx 0.004$ obtained from DMPC at 23°C (fig. 5b), i.e the system that is closest to phase transition ($T^* \approx 0$). In the gel phase, the observed $\Delta RP / RP < 0.001$ (the noise level) in DMPC at 10°C (fig. 5a). The intermediate response of $\Delta RP / RP \approx 0.0015$ is observed at 37°C (fig. 5c). Quantitatively similar response is seen when the state is changed by changing lipid composition at fixed temperature (fig 5). The system in gel state ($T^* < 0$), i.e. DPPC at 20°C (fig. 6a) gives $\Delta RP / RP < 0.001$ and DOPC at 20°C (fig. 6b) that is in fluid state ($T^* > 0$) gives an intermediate response of $\Delta RP / RP \approx 0.0015$. Clearly the response $\Delta RP / RP$ of the membrane is a function of state (here order parameter RP and temperature) and is not monotonic, for example with respect to T^* .

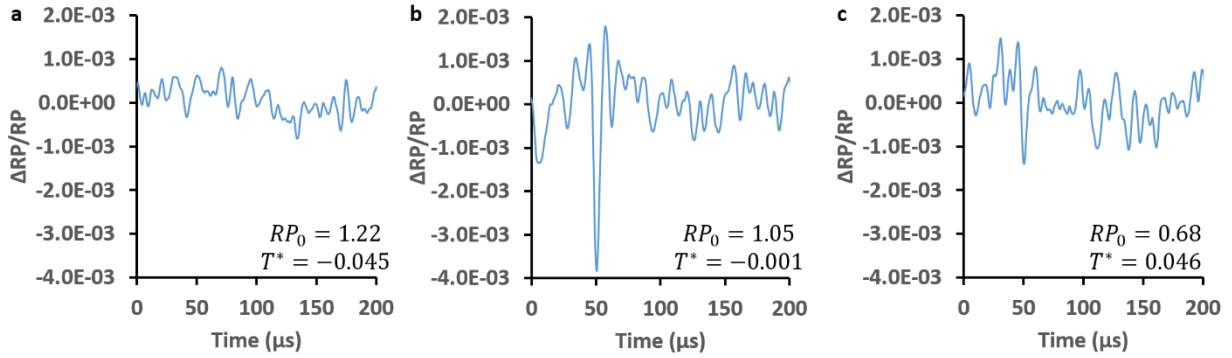


Figure 5 Perturbation response as a function of temperature *The average responses ($n=500$, Low-Pass 100kHz) are quantified by the change $\Delta RP/RP$ plotted as a function of time for DMPC MLVs at different temperatures, (a) 10°C, (b) 23°C, (c) 37°C*

To see if the values of $\Delta RP/RP$ make sense quantitatively, we look at $\Delta RP/RP \approx -0.004$ in the transition region. Based on general behavior of extensive observables near a transition, one can make the approximation $\Delta RP/RP \sim \Delta V/V$ [38], similar to discussion around eq.8. Typical volume increase associated with lipid phase transitions in DMPC under quasistatic conditions is known to be of the order of $\frac{\Delta V}{V} \approx 3\%$ [47,48]. Given that in same region the $\Delta RP/RP$ changes by -0.44 (fig. 4b), gives an average coupling coefficient in the transition region. Thermodynamically, the amplitude response in volume $\frac{\Delta V}{V}$ can be related to pressure amplitude in the linear approximation as $k_s = -\frac{\Delta V}{V} \frac{1}{\Delta P}$, where k_s is the adiabatic compressibility of the system. From measurements reported elsewhere, k_s would typically range from 3.1×10^{-10} to $5.27 \times 10^{-10} \text{ m}^2/N$, going from gel state to liquid state in DMPC MLVs [48]. Therefore the expected range for $\Delta RP/RP$, in region where $\Delta RP/RP = \text{const.} \cdot \Delta V/V$ is valid, would be from -0.004 to -0.007 . This fits the observation rather well given the first order nature of the calculation. Indeed, calculations based on adiabatic compressibility that were measured using low intensity ultrasound ($\sim 10^{-6} \text{ W/cm}^2$) are expected to overestimate the large amplitude response. Note that unlike the quasi-static case where the spectral width results from random thermal perturbations probing the specific heat of the system, the non-equilibrium nature of the acoustic response is captured by the adiabatic compressibility. The experiments essentially show the enhanced mechanical coupling between the

lipid interface and the sound waves near a transition as has previously been elaborated in by others [49].

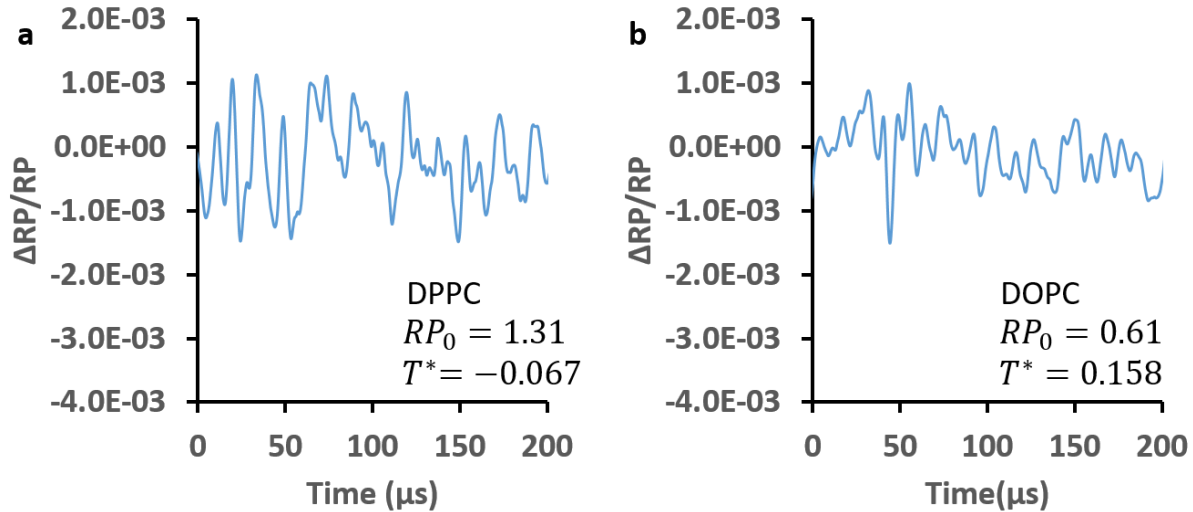


Figure 6 Perturbation response as a function of state *The average responses ($n=500$, Low-Pass 100kHz) are quantified by the change $\Delta RP/RP$ plotted as a function of time for the different MLV systems, (a) DPPC at 20°C and (b) DOPC at 20°C.*

The relaxation times in lipid membranes provide some insight into the waveform of the response. Experimentally distinct time scales have previously been identified by others in several different lipid systems when lipid vesicles were exposed to photo-thermal shocks (1°C temperature rise in 1ns) [50]. Broadly these time scales can be associated with formation of a kink in the lipid tail (1-10ns), rotation of lipids (100ns), lateral diffusion (1-10 μ s), formation of domains (100 μ s) and phase separation (>1ms). In comparison to the pressure front, the negative pressure tail of the impulse consists of longer time scales which are comparable to the lateral diffusion (1-10 μ s) range of the relaxation times in lipids. Changes in the lipid tail conformation (1-10ns) or rotation of lipids (100ns) that could happen in the pressure positive phase of the impulse would only alter the environment of the probe at lateral diffusion (1-10 μ s) timescale and hence a positive $\Delta RP/RP$ might not be observed at these timescales [50]. There is also the possibility of action of the impulse through water-to-vapor transition *near* the interface, which can take place in the expansion phase of the pulse. Indeed, at higher pressure amplitudes we observed clear signs of cavitation at the interface which will be discussed in a subsequent publication. The discussion here is limited to the

small amplitude pressure impulse where the membrane responds in accordance with the linear response theory, allowing quantitative predictions at infinitesimal amplitudes and correct orders of magnitude for finite amplitude pressure impulses, as discussed above.

Note that we have made no assumption regarding the nature of interaction between the fluorophore and membrane, e.g. whether it is “electro-chromic” or “solvato-chromic”. Still, while thermodynamics can explain the implications of a given value $\left(\frac{\partial T}{\partial \lambda}\right)^{-1}$ for the coupling term $\langle \delta \lambda \delta E \rangle$ but not why they couple, at least not without further knowledge on the structure of the molecules and *mechanistic* assumptions (placement and orientation vs hydration, charge interaction) about the nature of interaction between the fluorophore and its local environment. So when is the coupling between the energy distribution of the dye subsystem and its surrounding $\frac{\partial^2 S}{\partial E_1 \partial E_2} \delta E_1 \delta E_2$ in general, or $\left(\frac{\partial T}{\partial \lambda}\right)^{-1}$ significant? This is where a molecular model becomes important. A shift in emission or absorption maximum $h\Delta\nu$ of electro or solvato-chromatic dye is usually attributed to the work done by the transition dipole (emission) or ground state dipole (absorption) respectively, on the solvent environment, which is significant for charge-transfer probes due to stronger dipole interactions making them, for instance, “voltage sensitive” [51]. As a first order approximation $h\Delta\nu_{shift} = \Delta E_{solv} \sim \mathbf{F}_0 \cdot \Delta \mathbf{M}_{solv}$ is the electrical work done on the solvent in the frame of reference of the dye to reach the relaxed state, also known as solvent relaxation. Here \mathbf{F}_0 is average electric field of the ground state dipole (absorption) or of the transition dipole (emission) of the dye and $\Delta \mathbf{M}_{solv}$ is the change in average solvent dipole during solvation. Furthermore then $\langle \Delta E_{solv}^2 \rangle \sim \langle \Delta \mathbf{M}_{solv}^2 \rangle \sim T^2 \epsilon$, where ϵ is the dielectric constant of the interface analogous to solvent relaxation in bulk along the lines of Marcus and Fraunfelder [1,2,4,52]. Similarly, one should expect a pressure (\mathbf{P}) dependent change in the spectrum of a photoactive molecule $h\Delta\nu_{shift} = \Delta E_{solv} \sim \mathbf{P} \cdot \Delta \mathbf{V}_{solv}$ if it undergoes significant structural change and hence a volume change ($\Delta \mathbf{V}_{solv}$) on irradiation [53,54]. Indeed, molecules that can undergo photo isomerization (e.g. Azobenzene and its derivatives) show significant spectral shift as a function of pressure [55–57] and provide us with an avenue to develop “mechano-sensitive” dyes.

The relationships derived here attribute a thermodynamic meaning to the fluorescence spectra that significantly differs from how fluorescence data is currently interpreted in such systems [13]. Usually fluorescence spectra is interpreted in structural terms of “tight” packing of the molecule

into the bilayer and the resulting water content of its surroundings [39,58,59]. In model pure lipid vesicles, which show clear phase separation, the broadening during the transition can be partially attributed to the coexistence of the phase separated domains as given by the lever rule applied to a first order phase transition [13,21,60]. Multi-component system on the other hand can approach a critical limit where most of the molecules exist at a domain boundary [61] and in these systems the spectral fluctuation are expected to become evident at single molecule level [62] and can be investigated using, for instance, Fluorescence correlation spectroscopy (FCS) [63]. Interestingly in many biological systems, in the absence of direct evidence of phase separated domain like structures, fluorescence spectra show significant shift and state dependent broadening [18,22,64–66]. In these cases while the structural interpretation remains ambiguous, researchers are debating transient phase separated microdomains, known as lipid rafts [21,67], similar to fluctuating micro or nano domains that exist near a criticality [61] but are difficult to resolve experimentally. Eq. 1,3 and 9 presented here provide a thermodynamic meaning of the spectral fluctuations in terms of the thermodynamic susceptibility of the environment that does not require such a structural interpretation.

In fact, changes in the spectrum of Laurdan due to the introduction of other nonspecific molecules in the system, such as cholesterol, detergents, drugs, alcohol and other ingredients (Table 1) can also be explained similarly. State changes due to various molecular agents have been measured using Laurdan, they have been tabulated in Table 1 along with the corresponding references. Given that the presented theory unifies a wide extent of observations made with Laurdan in artificial systems, it remains to be seen how far these principles can be applied to dynamic process in Biology with all its heterogeneity intact. Experiments done previously on nerve fibers during an action-potential present a promising outlook, where the width of the emission spectrum was observed to shrink at the peak amplitude [68]. Independently, it has been shown using X-ray diffraction measurements that the nerve gets stiffer at the peak amplitude [69], as the work presented here would have predicted.

Therefore although the results based on artificial MLVs might appear to be rather specific to a particular lipid composition at a particular temperature and of little use in native biologic membranes with significant structural inhomogeneities, the generality becomes apparent when the system response is seen as a function of the thermodynamic state of the system and not that of the

structure [5]. Thus as seen in figure 5 and 6, it is not the molecular nature of the lipid but the thermodynamic state that is related to the observed perturbation of the dye spectrum in response to incident acoustic impulse. Such a thermodynamic state based perspective is also important given that native biological membranes self-organize and even adapt their composition to stay near a critical point in the state diagram of the biological membrane [64,70,71]. Laurdan has in fact been used in several of these studies showing that cell membranes change the lipid composition as they adapt to different environmental condition in order to stay in a relatively similar state near a transition [72]. Hence the contribution of the mechanism suggested here is expected to be significant in native biological membranes as well.

Conclusion

The energy spectrum of the dye Laurdan, embedded in a lipid membrane, has been shown to be a function of the state of the dye-membrane system. The width of the spectrum results from thermal fluctuations in the entropy potential of the coupled dye-membrane system. An acoustic impulse was used to probe the perturbation response of the dye and the magnitude of the response in either cases is shown to be related to the curvature of the potential or the thermodynamic susceptibilities. Due to the local nature of the fluorescence measurements, it should be possible to spatially resolve the heat capacity and other thermodynamic response functions of cellular microenvironments from fluorescence measurements [73]. The results suggest that fluorescence measurements in living systems can also provide insights into the role of state during adaptation [70,74] where the role of lipid transitions is well recognized [65,66,72], aging [75], and mechanotransduction [76]. Furthermore, these measurements will also help in determining the susceptibility of different cell types or a certain micro environment of theirs to pressure impulses (in general a perturbation in thermodynamic state) which in turn can help, for example, find better targets for acoustically triggered therapies.

Acknowledgement

S. Shrivastava and R. Cleveland are supported by Engineering and Physical Sciences Research Council (EPSRC) under Programme Grant EP/L024012/1 (OxCD3: Oxford Centre for Drug Delivery Devices).— The authors thank James Fisk and David Salisbury for constructing the water tank with the and shock wave setup. S. Shrivastava and M. Schneider thank Dr. Konrad Kaufmann (Göttingen), who introduced them to Einstein's approach to statistical physics recognizing its importance for biological physics. We also thank

him for numerous seminars and discussions. We would also like to thank Dr. Jeremy England and Dr. Christian Fillafer for their comments and suggestions.

	System	Agent for state change	Properties measured	Observation	Reference
1	Laurdan in lipid vesicles	Temperature, pH and lipid composition	Emission spectrum and GP (T)	(1) FWHM(T) _{max} in DPPC vesicles at 41C, coincides with PT of DPPC and [d(GP)/dT] _{max} . (2) [d(GP)/dT] _{max} indicates phase transition in vesicles of different lipid composition and different pH	[39]
2	Laurdan in DMPG vesicles in low ionic strength	Temperature	Emission spectrum and GP (T)	(1) DPMG at low ionic strength has a broad PT starting at 17C and peaking at 35C. (2) FWHM(T) _{max} around 35C which is in the PT region and near [d(GP)/dT] _{max} .	[16]
3	Laurdan in DPPC vesicles and Tamoxifen	Temperature, Tamoxifen concentration	Emission spectrum, GP(T), heat capacity C, Permeability	(1) Tamoxifen shifts DPPC PT and C _{max} from 41C to lower temperatures. (2) Shift in C _{max} due to tamoxifen coincides with shift in [d(GP)/dT] _{max} to 40C which is further consistent with increase in FWHM. (3) No effect of tamoxifen on FWHM at 35 and 50C as expected from [d(GP)/dT]~0 (4) Temperature and tamoxifen concentration corresponding to FWHM also results in maximum membrane permeability.	[77]
4	Laurdan and Prodan in DSPC vesicles	Pressure and Temperature	Emission Spectrum	(1) FWHM for both Laurdan and Prodan, as a function of pressure, has a maximum at the pressure induced order disorder transition at 63C. (2) Only the FWHM of Prodan has a maximum at pressure induced inter-digitated crystalline state at 49C while Laurdan is insensitive.	[17]
5	Prodan in DPPC	Cholesterol and Ethanol	Emission Spectrum	(1) FWHM as a function of cholesterol concentration has a maximum at 15% and 50C. Independently this coincides with the corresponding order-disorder transition in the DPPC/cholesterol phase diagram(82)	[27]
6	Laurdan in POPC and DPPC	Temperature and @-Tocopherol	Emission Spectrum	@-Tocopherol influences FWHM in POPC at 25C as [d(GP)/dT]#0 but not in DPPC as [d(GP)/dT]~0 at 25C	[78]
7	Laurdan in pig kidney basolateral membrane	Cholesterol	GP as a function of cholesterol concentration	Maximum N ⁺ /K ⁺ -ATPase activity coincides with cholesterol concentration corresponding to (d(GP)/d[cholesterol]) _{max}	(69)
8	Laurdan in lipid extracts from human skin stratum corneum (HSC) and bovine brain (BB)	Temperature, pH, lipid composition	GP (T), C(T)	C(T) _{max} coincides with [d(GP)/dT] _{max} for HSC extracts but not for BB extracts, again indicating that Laurdan might not be suitably located to detect all transitions.	[80]
9	Laurdan in plasma membrane from rat brain cortex	Concentration of Brij58, Triton and Digitonin	Emission Spectra and G-protein activity	(1) Brij 58 and Triton induce a state of increased FWHM while Digitonin does not. (2) Brij58 and Triton concentrations corresponding to FWHM _{max} induce maximum increase in G protein activity while Digitonin does not.	[18]
10	Laurdan in HIV virus	Methyl-β-cyclodextrin and temperature	Emission spectrum	FWHM _{max} coincides with [d(GP)/dT] _{max}	[22]
11	Laurdan in brain phosphatidyl serine	Calcium concentration	Excitation and emission spectrum	Narrowing of the spectrum coincides with a blue shift on addition of calcium	[81]

12	Laurdan in Escherichia Coli	Temperature and Chloramphenicol (cam)	Emission Spectra, steady state and time resolved	Peak in $[d(GP)/dT]$ near physiological temperature which shifts to lower temperature on cam treatment. Narrowing of the emission spectra on cooling.	[65]
13	Laurdan in Rat liver microzomes	Temperature and fatty acids	Emission Spectra and GP	Significant narrowing and blue shift in spectra as a function of temperature	[82]

Table 1. Summarizing the experimental studies supporting the derived relationship between fluorescence spectra of an embedded dye and membrane susceptibility. GP represents generalized polarization, C represents heat capacity of the entire sample. GP(T) or C(T) for e.g. implies measured as a function of temperature.

References

- [1] P. W. Fenimore, H. Frauenfelder, B. H. McMahon, and R. D. Young, Proc. Natl. Acad. Sci. **101**, 14408 (2004).
- [2] H. Frauenfelder, G. Chen, J. Berendzen, P. W. Fenimore, H. Jansson, B. H. McMahon, I. R. Stroe, J. Swenson, and R. D. Young, Proc. Natl. Acad. Sci. U. S. A. **106**, 5129 (2009).
- [3] R. a. Marcus, J. Chem. Phys. **24**, 979 (1956).
- [4] R. A. Marcus and A. Amos, **811**, 265 (1985).
- [5] M. Schneider, Thermodynamic States and Transitions as the Foundation of Biological Functions: Self-Organized Blood and Einstein ' S View on Soft Interfaces, University of Augsburg, 2011.
- [6] K. Kaufmann, *On the Role of Phospholipid Membrane in Free Energy Coupling*, 1st ed. (Caruaru, Brasil, 1989).
- [7] A. Einstein, Ann. Phys. **4**, 513 (1901).
- [8] S. S. L. Andersen, A. D. Jackson, and T. Heimburg, Prog. Neurobiol. **88**, 104 (2009).
- [9] S. Shrivastava and M. F. Schneider, J. R. Soc. Interface **11**, (2014).
- [10] J. Griesbauer, S. Bössinger, a. Wixforth, and M. Schneider, Phys. Rev. E **86**, 61909 (2012).
- [11] B. Wunderlich, C. Leirer, A. Idzko, U. F. Keyser, A. Wixforth, V. M. Myles, and T. Heimburg, Biophysj **96**, 4592 (2009).
- [12] T. Franke, C. T. Leirer, A. Wixforth, N. Dan, and M. F. Schneider, Chemphyschem **10**, 2852 (2009).
- [13] T. Parasassi, G. De Stasio, a d'Ubaldo, and E. Gratton, Biophys. J. **57**, 1179 (1990).
- [14] M. Viard, J. Gallay, M. Vincent, O. Meyer, B. Robert, and M. Paternostre, Biophys. J. **73**, 2221 (1997).
- [15] M. Viard, J. Gallay, M. Vincent, and M. Paternostre, Biophys. J. **80**, 347 (2001).

- [16] A. D. Lúcio, C. C. Vequi-Suplicy, R. M. Fernandez, and M. T. Lamy, *J. Fluoresc.* **20**, 473 (2010).
- [17] M. Kusube, N. Tamai, H. Matsuki, and S. Kaneshina, *Biophys. Chem.* **117**, 199 (2005).
- [18] J. Sýkora, L. Bourová, M. Hof, and P. Svoboda, *Biochim. Biophys. Acta* **1788**, 324 (2009).
- [19] A. Szilágyi, E. Selstam, and H.-E. Akerlund, *Biochim. Biophys. Acta* **1778**, 348 (2008).
- [20] C. C. De Vequi-Suplicy, C. R. Benatti, and M. T. Lamy, *J. Fluoresc.* **16**, 431 (2006).
- [21] S. a Sanchez, M. a Tricerri, and E. Gratton, *Proc. Natl. Acad. Sci. U. S. A.* **109**, 7314 (2012).
- [22] M. Lorizate, B. Brügger, H. Akiyama, B. Glass, B. Müller, G. Anderluh, F. T. Wieland, and H.-G. Kräusslich, *J. Biol. Chem.* **284**, 22238 (2009).
- [23] D. M. Owen, P. M. P. Lanigan, C. Dunsby, I. Munro, D. Grant, M. A. A. Neil, P. M. W. French, and A. I. Magee, *Biophys. J.* **90**, L80 (2006).
- [24] Y. Wang, G. Jing, S. Perry, F. Bartoli, and S. Tatic-Lucic, *Opt. Express* **17**, 984 (2009).
- [25] D. M. Owen and K. Gaus, *Microsc. Res. Tech.* **9999**, 1 (2009).
- [26] T. Parasassi, E. Krasnowska, L. a Bagatolli, and E. Gratton, *J. Fluoresc.* **8**, 365 (1998).
- [27] O. P. Bondar and E. S. Rowe, *Biophys. J.* **76**, 956 (1999).
- [28] R. J. Clarke and D. J. Kane, *Biochim. Biophys. Acta* **1323**, 223 (1997).
- [29] S. Chowdhury and B. Chanda, *J. Gen. Physiol.* **140**, 613 (2012).
- [30] A. Einstein, in *Collect. Pap. Albert Einstein* (Princeton University Press, 1911), p. 427.
- [31] A. Einstein, *Ann. Phys.* **33**, 1275 (1910).
- [32] H. Jaffe and A. Miller, *J. Chem. Educ.* **43**, 469 (1966).
- [33] S. Mashimo, S. Kuwabara, S. Yagihara, and K. Higasi, *J. Phys. Chem.* **91**, 6337 (1987).
- [34] A. Einstein, *Ann. Phys.* **10**, 183 (1909).
- [35] P. Grabitz, V. P. Ivanova, and T. Heimburg, *Biophys. J.* **82**, 299 (2002).
- [36] D. Steppich, J. Griesbauer, T. Frommelt, W. Appelt, a. Wixforth, and M. Schneider, *Phys. Rev. E* **81**, 1 (2010).
- [37] T. Heimburg, *Biochim. Biophys. Acta - Biomembr.* **1415**, 147 (1998).
- [38] S. Shrivastava and M. F. Schneider, *PLoS One* **8**, 2005 (2013).
- [39] T. Parasassi, G. De Stasio, G. Ravagnan, R. M. Rusch, and E. Gratton, *Biophys. J* **60**, 179 (1991).
- [40] T. Y. Titova, V. Y. Artyukhov, O. M. Zharkova, and J. P. Morozova, *Spectrochim. Acta - Part A Mol. Biomol. Spectrosc.* **124**, 64 (2014).
- [41] D. A. Wilkinson and J. F. Nagle, *Biochim. Biophys. Acta - Biomembr.* **688**, 107 (1982).
- [42] A. Poperscu, M. Radu, B. Zorilla, and M. Bacalum, *Optoelectron. Adv. Mater. - Rapid Commun.* **7**, 456 (2013).
- [43] D. Papahadjopoulos and M. Moscarello, *Biochim. Biophys. ...* **401**, 317 (1975).

- [44] S. Shrivastava and M. F. Schneider, *J. R. Soc. Interface* **11**, 1 (2014).
- [45] D. Needham and E. Evans, *Biochemistry* **27**, 8261 (1988).
- [46] A. S. Ulrich, M. Sami, and A. Watts, *BBA - Biomembr.* **1191**, 225 (1994).
- [47] S. Halstenberg, T. Heimburg, T. Hianik, U. Kaatz, and R. Krivanek, *Biophys. J.* **75**, 264 (1998).
- [48] R. Krivanek, L. Okoro, and R. Winter, *Biophys. J.* **94**, 3538 (2008).
- [49] D. B. Tatat and F. Dunn, *J. Phys. Chem.* 3548 (1992).
- [50] J. Holzwarth, in edited by A. Cooper, J. Houben, and L. Chien, *Proceeding (Springer Science + Buisness Media, LLC, New York, 1989)*.
- [51] G. Bublitz and S. Boxer, *Annu. Rev. Phys. Chem.* **48**, 213 (1997).
- [52] M. K. Prakash and R. a Marcus, *Proc. Natl. Acad. Sci. U. S. A.* **104**, 15982 (2007).
- [53] H. Frauenfelder, N. a Alberding, A. Ansari, D. Braunstein, B. R. Cowen, M. K. Hong, I. E. T. Iben, J. B. Johnson, S. Luck, M. C. Marden, J. R. Mourant, P. Ormos, L. Reinisch, R. Scholl, A. Schulte, E. Shyamsunder, L. B. Soremen, P. J. Steinbach, A. Xie, and R. D. Young, *J. Phys. Chemsitry* **94**, 1024 (1990).
- [54] K. Mairing, J. Deich, F. I. Rosell, T. B. McAnaney, W. E. Moerner, and S. G. Boxer, *J. Phys. Chem. B* **109**, 12976 (2005).
- [55] A. H. Kadhim, **973**, 1805 (1966).
- [56] M. Shimomura and T. Kunitake, **33**, 5175 (1987).
- [57] T. Asano and T. Okada, *J. Org. Chem.* **49**, 4387 (1984).
- [58] L. Bagatolli, *Chem. Phys. Lipids* **122**, 137 (2003).
- [59] F. M. Harris, K. B. Best, and J. D. Bell, *Biochim. Biophys. Acta* **1565**, 123 (2002).
- [60] T. Parasassi, G. Ravagnan, R. M. Rusch, and E. Gratton, *Photochem. Photobiol.* **57**, 403 (1993).
- [61] A. R. Honerkamp-Smith, P. Cicuta, M. D. Collins, S. L. Veatch, M. den Nijs, M. Schick, and S. L. Keller, *Biophys. J.* **95**, 236 (2008).
- [62] T. Wazawa, Y. Ishii, T. Funatsu, T. Yanagida, T. O. Baldwin, J. A. Christophore, F. M. Raushel, J. F. Sinclair, M. M. Ziegler, A. J. Fisher, I. Rayment, R. M. Dickson, A. B. Cubitt, R. Y. Tsien, W. E. Moerner, R. M. Dickson, D. J. Norris, Y.-L. Tzeng, W. E. Moerner, T. Funatsu, Y. Harada, M. Tokunaga, K. Saito, T. Yanagida, T. Ha, T. Enderle, D. F. Ogletree, D. S. Chemla, P. R. Selvin, S. Weiss, T. Ha, A. Y. Ting, J. Liang, W. B. Caldwell, A. A. Deniz, D. S. Chemla, P. G. Schultz, S. Weiss, Y. Harada, K. Sakurada, T. Aoki, D. D. Thomas, T. Yanagida, Y. Ishii, T. Funatsu, T. Wazawa, T. Yoshida, J. Watai, M. Ishii, T. Yanagida, T. Ishii, T. Funatsu, T. Yoshida, T. Wazawa, T. Yanagida, A. Ishijima, H. Kojima, T. Funatsu, M. Tokunaga, H. Higuchi, H. Tanaka, T. Yanagida, Y. Itoh, K. Kamasaki, J. Iwahara, T. Terada, A. Kamiya, M. Shirouzu, Y. Muto, G. Kawai, S. Yokoyama, E. D. Laue, M. Wälchli, T. Shibata, S. Nishimura, T. Miyazawa, F. Jelezko, P. Tamarat, B. Lounis, M. Orrit, M. Klessinger, J. Michl, J. F. Koretz, L. M. Coluccio, A. M. Bertasso, S. Lowey, H. S. Slayter, A. G. Weeds, H. Baker, H. P. Lu, X. S. Xie, H. P. Lu, L. Xun, X. S. Xie, J. J. Macklin, J. K. Trautman, T. D. Harris, L. E. Brus, K.-M. Pan, M.

- Baldwin, J. Nguyen, M. Gasset, A. Serban, D. Groth, I. Mehlhorn, Z. Huang, R. J. Fletterick, F. E. Cohen, S. B. Prusiner, S. V. Perry, E. J. Sánchez, L. Novotny, G. R. Holtom, X. S. Xie, I. Sase, H. Miyata, S. Ishiwata, K. Kinoshita, T. Schmidt, G. J. Schütz, W. Baumgartner, H. J. Gruber, H. Schindler, U. P. Shinde, J. J. Liu, M. Inouye, J. L. Sohl, S. S. Jaswal, D. A. Agard, M. Tokunaga, K. Kitamura, K. Saito, A. H. Iwane, T. Yanagida, J. K. Trautman, J. J. Macklin, L. E. Brus, E. Betzig, R. D. Vale, T. Funatsu, D. W. Pierce, L. Romberg, Y. Harada, T. Yanagida, Z. Wang, J. Mottonen, E. J. Goldsmith, D. M. Warshaw, E. Hayes, D. Gaffney, A.-H. Lauzon, J. Wu, G. Kennedy, K. Trybus, S. Lowey, C. Berger, K. D. Weston, P. J. Carson, H. Metiu, S. K. Buratto, X.-H. Xu, E. S. Yeung, T. Yamashita, Y. Soma, S. Kobayashi, and T. Sekine, *Biophys. J.* **78**, 1561 (2000).
- [63] R. Rigler, *Biochem. Biophys. Res. Commun.* **396**, 170 (2010).
- [64] J. R. Hazel, S. J. McKinley, and M. F. Gerrits, *Am. J. Physiol.* **275**, R861 (1998).
- [65] S. Vanounou, D. Pines, E. Pines, A. H. Parola, and I. Fishov, *Photochem. Photobiol.* **76**, 1 (2002).
- [66] T. Toyoda, Y. Hiramatsu, T. Sasaki, and Y. Nakaoka, *J. Exp. Biol.* **212**, 2767 (2009).
- [67] S. Munro, *Cell* **115**, 377 (2003).
- [68] I. Tasaki, E. Carbone, K. Sisco, and I. Singer, *Biochim. Biophys. Acta (BBA ...)* **323**, 220 (1973).
- [69] V. Luzzati, L. Mateu, G. Marquez, and M. Borgo, *J. Mol. Biol.* **286**, 1389 (1999).
- [70] J. Hazel, *Annu. Rev. Physiol.* **19** (1995).
- [71] D. Melchior and J. Steim, *Annu. Rev. Biophys. Bioeng.* **5**, 205 (1976).
- [72] T. Sasaki, Y. Konoha, T. Toyoda, Y. Yasaka, E. Przybos, and Y. Nakaoka, *J. Exp. Biol.* **209**, 3580 (2006).
- [73] E. Sezgin, D. Waithe, J. Bernardino De La Serna, and C. Eggeling, *ChemPhysChem* **16**, 1387 (2015).
- [74] a R. Cossins and C. L. Prosser, *Proc. Natl. Acad. Sci. U. S. A.* **75**, 2040 (1978).
- [75] T. Parasassi, M. Di Stefano, G. Ravagnan, O. Saporita, and E. Gratton, *Exp. Cell Res.* **202**, 432 (1992).
- [76] K. Yamamoto and J. Ando, *J. Cell Sci.* **126**, 1227 (2013).
- [77] M. Engelk, P. Bojarski, R. Bloss, and H. Diehl, *Biophys. Chem.* **90**, 157 (2001).
- [78] J. B. Massey, *Chem. Phys. Lipids* **109**, 157 (2001).
- [79] C. P. Sotomayor, L. F. Aguilar, F. J. Cuevas, M. K. Helms, and D. M. Jameson, *Biochemistry* **39**, 10928 (2000).
- [80] I. Plasencia, L. Norlén, and L. a Bagatolli, *Biophys. J.* **93**, 3142 (2007).
- [81] K. Ramani and S. V Balasubramanian, *Biochim. Biophys. Acta - Biomembr.* **1618**, 67 (2003).
- [82] H. a Garda, a M. Bernasconi, R. R. Brenner, F. Aguilar, M. a Soto, and C. P. Sotomayor, *Biochim. Biophys. Acta* **1323**, 97 (1997).